Atomic order and magnetization distribution in the half metallic and nearly half metallic $C1_b$ compounds NiMnSb and PdMnSb



2010 J. Phys.: Condens. Matter 22 206004

(http://iopscience.iop.org/0953-8984/22/20/206004)

J. Phys.: Condens. Matter **22** (2010) 206004 (6pp) doi:10.1088/0953-8984/22/20/206004

# Atomic order and magnetization distribution in the half metallic and nearly half metallic $C1_b$ compounds NiMnSb and PdMnSb

**P J Brown[1,2], A P Gandy[1], R Kainuma[3], T Kanomata[4], T Miyamoto[3], M Nagasako[3], K U Neumann[1], A Sheikh[1] and K R A Ziebeck[5]**

[1] Department of Physics, Loughborough University, LE11 3TU, UK
[2] Institut Laue Langevin, BP 156, 38042 Grenoble, France
[3] Institute of Multidisciplinary Research for Advanced Materials, Tohoku University, 2-1-1 Katahira, Sendai 980-8577, Japan
[4] Faculty of Engineering, Tohoku Gakuin University, Tagajo 985-8537, Japan
[5] Cavendish Laboratory, Cambridge University, Madingley Road, CB3 0HE, UK

Received 15 March 2010, in final form 31 March 2010
Published 26 April 2010
Online at stacks.iop.org/JPhysCM/22/206004

**Abstract**
Polarized neutron diffraction has been used to study the magnetization distribution in two isostructural inter-metallic compounds NiMnSb and PdMnSb. Band structure calculations have predicted that whereas the former should be a half metallic ferromagnet the latter should not. Measurements made at 5 K on different crystals show that disorder can occur between the A (Mn) and B (Sb) sites in both alloys and in the case of NiMnSb, by partial occupation of the void D sites by Ni. In all the crystals most of the moment was found on the Mn atoms in the A sites; in NiMnSb it is due to spin only but in PdMnSb there is evidence for a significant orbital contribution ($g = 2.22$). The magnitudes of the moments associated with each atom are in fair agreement with the theoretical values; however, the distribution of magnetization around the Mn atoms is found to have nearly spherical symmetry (40% $e_g$) rather than the 50% $e_g$ character expected from the band structure.

## 1. Introduction

The possibility of using selectivity of the electronic spin in semiconductor devices (spintronics) is currently attracting considerable attention [1]. Possible applications are: to increase giant magneto-resistance (GMR), as spin injector electrodes in tunnel magneto-resistance (TMR) structures, or for introducing spin polarized currents into semiconductors. Such devices require the injection of a spin polarized current and substantial efforts are being made to find the so-called half metallic ferromagnets capable of providing such currents. Half metallic ferromagnets are a relatively new class of material [2] which have an energy gap at the Fermi energy between the majority and minority spin bands, as shown in figure 1(a), leading to properties which are of both fundamental and technological interest. The presence of the gap influences the transport properties and restricts low temperature magnetic fluctuations to just the spin waves, as shown in figure 1(b.) With increasing temperature, transitions across the gap between the majority and minority bands can

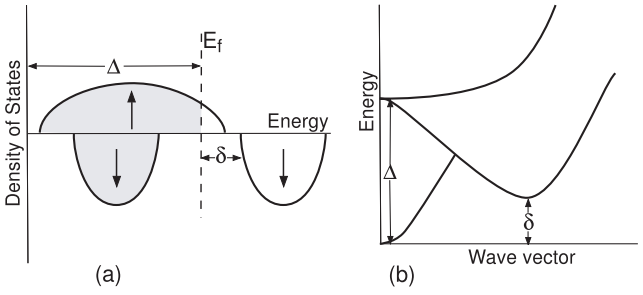


**Figure 1.** (a) Schematic band structure of a half metallic ferromagnet. (b) Spectrum of magnetic excitations in a half metallic ferromagnet.

 

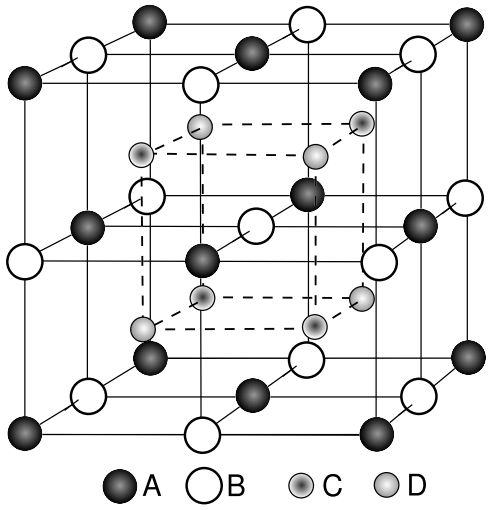


**Figure 2.** Unit cell of the $L2_1$ Heusler alloy structure. In the ideal $C1_b$ structure the D sites are vacant.

occur; changing both the magnetization distribution and the transport properties.

The family of ferromagnetic alloys XYZ, in which X and Y are transition metals and Z is a B sub-group element, and which crystallize with the $C1_b$ structure illustrated in figure 2 may have the required band structure. The possibility of half metallic behaviour in $C1_b$ compounds was first recognized in band structure calculations using the augmented spherical wave method [2]. The striking difference found between the bands for the majority and minority spin states was attributed to broken conjugation symmetry due to the non-centrosymmetric $C1_b$ space group ($F\bar{4}3m$). In this and subsequent band structure calculations [3, 4] the gap in the minority spin states is shown to originate from strong hybridization between the d states of the two transition metal atoms and is intimately connected to the $C1_b$ crystal structure. The gap lies between the 3d bonding and antibonding bands and in NiMnSn is estimated to be 0.5 eV at 0 K. In the majority spin bands hybridization between Sb p and Mn $t_{2g}$ states leads to a broad conduction band which intersects the Fermi surface.

Systematic band structure calculations [5] for a number of $C1_b$ systems have shown that the half metallic property is lost when reduced overlap between $t_{2g}$ states of the metal atoms due to increasing lattice parameter narrows the energy gap in the minority spin states so that the Fermi level falls either above or below the energy gap. The calculations confirm that NiMnSb should be half metallic whereas in PdMnSb, with a substantially larger lattice parameter, the Fermi level in the minority spin band lies near the top of the $t_{2g}$ bonding band.

Although band structure calculations predict that ferromagnetic compounds with the $C1_b$ structure are ideal half metallic magnets and a gap in the minority spins states in NiMnSb and PtMnSb has been confirmed by experiment [6, 7] the possibility of producing spin polarized currents still awaits experimental verification. Many experiments carried out up to now are surface or interface sensitive, probing a region where the half metallic property is reported to be lost. Neutron diffraction enables the bulk of a sample to be probed and

**Table 1.** Some physical properties of NiMnSb and PdMnSb [12].

| Alloy | Structure | Lattice constant (Å) | Curie temp. (K) | Magnetic moment ($\mu_B$/f.u.) |
|---|---|---|---|---|
| NiMnSb | $C1_b$ | 5.909 | 730 | 3.85 |
| PdMnSb | $C1_b$ | 6.248 | 500 | 3.95 |

if polarized neutrons are employed the relative occupations of bands of different symmetries giving rise to the magnetic moment can be established. Such results provide alternative information which can be use to test the validity of the band structure calculations. Polarized neutron measurements made on $CoS_2$ [8] and some Heusler alloys [9] show that none of these materials have the half metallic character that had been predicted.

The present paper reports the results of a polarized neutron diffraction study of $C1_b$ alloys in which the magnetization distributions in PdMnSb and in two NiMnSb samples with different degrees of atomic order have been determined and are compared. Some polarized neutron scattering measurements have already been made on both NiMnSb [10] and PdMnSb [11] but in neither case was the extent of the data collected or the methods used in the analysis of the results sufficient to characterize the bands giving rise to the magnetization.

## 2. Physical properties

Both NiMnSb and PdMnSb crystallize with the cubic non-centrosymmetric $C1_b$ structure which has space group $F\bar{4}3m$. The structure, which is shown in figure 2, is closely related to that of the Heusler alloys ($L2_1$) except that one of the four sublattices is void. A summary of the bulk properties of both alloys is given in table 1 [12].

## 3. Experimental details

### *3.1. Specimen preparation*

Crystals of NiMnSb (B) and PdMnSb were initially grown using the Bridgeman technique. The resulting boules were not single crystals but contained several large grains. After etching and examination using the neutron Laue technique (The Orient Express instrument at ILL) samples approximately $2 \times 2 \times 6$ mm$^3$ were cut from the ingots in which the long axis was parallel to $\langle 1\bar{1}0 \rangle$. A second single crystal of NiMnSb (A) was obtained by a grain growth method in which the specimen was annealed at 1000 °C for 60 days in an argon atmosphere. A rectangular parallelepiped specimen of similar size and orientation was spark eroded from the ingot.

### *3.2. Unpolarized neutron diffraction*

The crystals were mounted successively on D9 in a four-circle Joule–Thomson refrigerator and cooled to 4 K. The integrated intensities of reflections with $\sin\theta/\lambda \leqslant 1.0$ Å$^{-1}$ were measured at a neutron wavelength of 0.84 Å. Those

with $\sin\theta/\lambda \leqslant 0.7$ Å$^{-1}$ were also measured at the shorter wavelength 0.51 Å. After averaging over symmetrically equivalent intensities, experimental structure factors were calculated from the data. A preliminary structure refinement suggested that the PdMnSb crystal and NiMnSb(A) were nearly completely ordered whereas NiMnSb(B) was partly disordered. All three crystals showed significant extinction, giving a reduction in intensity of ≈30% in the strongest reflections.

### 3.3. Polarized neutron diffraction

Flipping ratio measurements were made on these same crystals, mounted with $\langle 1\bar{1}0\rangle$ axes parallel to the polarization direction, using the polarized neutron diffractometer D3 at ILL. The crystals were held at 4 K in a vertical magnetizing field of 4 T provided by a cryomagnet. All accessible reflections with $h$–$k \leqslant 2$ and $\sin\theta/\lambda \leqslant 1.0$ Å$^{-1}$ were measured with a wavelength 0.825 Å. Where possible, four symmetrical equivalents of each independent reflection were included. The stronger low angle reflections were re-measured using a wavelength 0.54 Å.

### 3.4. Magnetization measurements

The magnetization of the crystals used in diffraction measurements was measured as a function of applied field at 5 K using a superconducting quantum interference device (SQUID) magnetometer. The results showed that the magnetization of both NiMnSb and PdMnSb was saturated at fields above 1.5 T at values of 94.4(2) and 87.4(6) J T$^{-1}$ kg$^{-1}$, respectively. These correspond to saturated moments of 3.957(8) $\mu_B$/f.u. for NiMnSb and 3.92(2) $\mu_B$/f.u. for PdMnSb.

## 4. Data analysis

### 4.1. Integrated intensities

Both PdMnSb and NiMnSb have the half Heusler C1$_b$ structure, space group $F\bar{4}3m$ (figure 2). In this arrangement there are only four different types of structure factor:

$$\begin{aligned}
&\text{Type 1} \quad h,k,l \text{ all even } h+k+l = 4n\\
&\quad F_1 = 4(b_A + b_B + b_C + b_D)\\
&\text{Type 2} \quad h,k,l \text{ all even } h+k+l = 4n+2\\
&\quad F_2 = 4(b_A + b_B - b_C - b_D)\\
&\text{Type 3} \quad h,k,l \text{ all odd } h+k+l = 4n+1\\
&\quad F_3 = 4(b_A - b_B) + 4\imath(b_C - b_D)\\
&\text{Type 4} \quad h,k,l \text{ all odd } h+k+l = 4n+3\\
&\quad F_4 = 4(b_A - b_B) - 4\imath(b_C - b_D).
\end{aligned} \tag{1}$$

The last two are complex conjugate to one another and give the same intensity. It is therefore usually not possible to determine the site scattering lengths uniquely from intensity measurements alone. The ratio $(b_C + b_D)/(b_A + b_B)$ can be obtained by combining type 1 and type 2 reflections but type 3 and 4 reflections only impose certain limits on the differences $b_A - b_B$ and $b_C - b_D$. The assumption that the D sites are empty gave reasonable fits to the integrated intensity measurements but indicated that although the PdMnSb and NiMnSb(A) crystals were reasonably well ordered, the NiMnSb(B) crystal had significant disorder.

### 4.2. Polarized neutron asymmetries

The C1$_b$ structure is non-centrosymmetric and, as indicated previously, the site occupancies and hence the nuclear structure factors cannot be determined uniquely from integrated intensity measurements. It is, therefore, not possible to extract the magnetic structure factors directly from the measured flipping ratios. For a Bragg reflection with nuclear and magnetic structure factors $N = N' + \imath N''$ and $M = M' + \imath M''$ whose scattering vector is inclined at an angle $\rho$ to the magnetization direction:

$$\begin{aligned}
R &= \frac{I^+}{I^-}\\
&= \frac{|N|^2 + |M|^2\cos^2\rho + P^+(M'N' + M''N'')\cos^2\rho}{|N|^2 + |M|^2\cos^2\rho + P^-(M'N' + M''N'')\cos^2\rho}.
\end{aligned}$$

It is more convenient in this case to work with *polarized neutron intensity asymmetries*

$$\begin{aligned}
A &= \frac{I^+ - I^-}{I^+ - I^-} = \frac{(P^+ - P^-)(M'N' + M''N'')\cos^2\rho}{(P^+ + P^-)(|N|^2 + |M|^2\cos^2\rho)}\\
&= \frac{R-1}{R+1}.
\end{aligned}$$

Use of $A$ allows the data to be corrected for the polarizing efficiency and averages to be made of equivalent reflections measured with the same $\rho$ before starting a fitting procedure.

Using the polarized neutron asymmetries goes some way towards resolving the ordering uncertainty; the asymmetries for the four types of reflection are:

$$\begin{aligned}
&\text{Type 1} \quad A = 2(\mu_A f_A + \mu_B f_B + \mu_C f_C + \mu_D f_D)/F_1\\
&\text{Type 2} \quad A = 2(\mu_A f_A + \mu_B f_B - \mu_C f_C - \mu_D f_D)/F_1\\
&\text{Types 3, 4} \quad A = 2[(\mu_A f_A - \mu_B f_B)(b_A - b_B)\\
&\qquad + (\mu_C f_C - \mu_D f_D)(b_C - b_D)]/|F_3|^2
\end{aligned} \tag{2}$$

where $\mu_X$ is the moment on site X and $f_X$ its magnetic form factor.

Although again there are only three independent equations and four unknown site moments the functional dependence of the structure factors and the asymmetries on the site parameters are rather different from those of the squared structure factors. Including both structure amplitudes and asymmetries in a least squares refinement gives a least squares matrix which is not quite singular; it has very large off-diagonal terms corresponding to high correlation between certain parameters and leads to unstable refinements. To avoid this problem some physically reasonable constraints have to be imposed on the parameters. The preliminary structure refinements showed that in all cases the ratio $F = (b_C + b_D)/(b_A + b_B)$ was high (5.4–5.6). Assuming stoichiometry this gives $b_A + b_B = 1.84$–$1.87$ fm, and $b_C + b_D = 10.2$–$10.3$ fm, these values can only

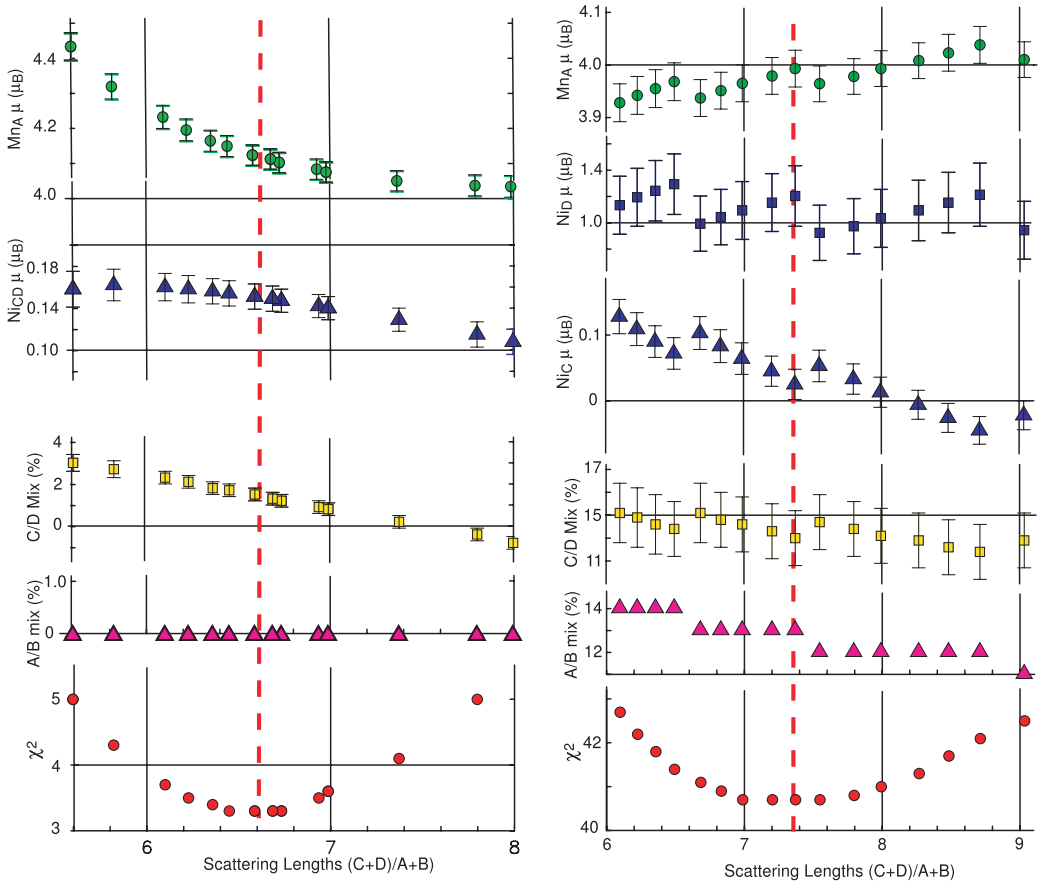


**Figure 3.** Variation with $F = (b_C + b_D)/(b_A + b_B)$ of the goodness of fit $\chi^2$ obtained in refinements of the model structures of NiMnSb (crystals A and B) using both integrated intensities and polarized asymmetries as data. The variation of values of the refined parameters are also shown.

(This figure is in colour only in the electronic version)

be obtained if nearly all the Ni is on the C and D sites. There can be up to 4% Mn in vacant C or D sites or up to 3% mixing between Sb and Ni. A model was elaborated in which most of the Mn and Sb is distributed over the A and B sites and most of the Ni is on the C and D sites with $F$ in the range 5.3–5.7. Fractional disorder $d_{AB}$ between the A and B sites and $d_{CD}$ between the C and D sites gives

$$b_A - b_B = \frac{b_A + b_B}{b_{Mn} + b_{Sb}}(1 - 2d_{AB})(b_{Mn} - b_{Sb})$$

$$b_C - b_D = (b_C + b_D)(1 - 2d_{CD}).$$

There are moments $\mu_{MnA}$, $\mu_{MnB}$ on each Mn atom in the A and B sites and moments $\mu_{NiC}$, $\mu_{NiD}$ on each atom in the C and D sites, respectively. This model was refined collectively with the integrated intensity and polarized neutron asymmetries for a range of fixed values of $R$ and $d_{AB}$. The parameters varied were $d_{CD}$, $\mu_{MnA}$, $\mu_{MnB}$, $\mu_{NiC}$, $\mu_{NiD}$, four isotropic site temperature factors, a scale factor for each of the two sets of integrated intensity data and a single extinction parameter; the mosaic spread parameter in the Becker Coppens model for type I crystals [13]. The goodness of fit was measured by

$$\chi^2 = \frac{1}{J}\sum_{j=1}^{j=J}\frac{1}{I - N_{pars}}\sum_{i=0}^{i=I}\left(\frac{(x_{obs}^{ji} - x_{calc}^{ji})}{\sigma(x_{obs}^{ji})}\right)^2$$

where $x_{obs}^{ji}$ is the value of the $i$th observation in the $j$th data set, $x_{calc}^{ji}$ its calculated value and $\sigma(x_{obs}^{ji})$ its estimated standard deviation. $N_{pars}$ is the number of parameters fitted. It was found that it was not possible to refine the moments on Ni or Mn for sites with less that 10% occupancy and these were fixed to zero. For each value of $F$ the $d_{AB}$ which gave the lowest $\chi^2$ was chosen. Figure 3 shows the results for the two NiMnSb crystals; the refined values of $d_{CD}$, $\mu_{NiC}$, $\mu_{NiD}$ and $\mu_{Mn}$ are plotted against $F$. It can be seen that these parameters vary by not much more than their standard deviations around the minimum in $\chi^2$. The site scattering lengths and the corresponding site occupancies (Occ) together with the magnetic moment values derived in this way are shown in table 2.

### *4.3. Magnetization distribution*

The site occupation parameters, isotropic temperature factors and the extinction parameters derived from the best fits described above were used and fixed in refinements of all the data using a model in which the magnetization distribution is given by the sum of atomic magnetization distributions associated with each magnetic atom. The atomic

**Table 2.** Parameters for the models giving the best fit with the integrated intensity and polarized neutron data for PdMnSb and NiMnSb (crystals A and B).

| Site | | PdMnSb | NiMnSb (A) | NiMnSb (B) |
|---|---|---|---|---|
| A | $b$ (fm) | −2.62(2) | −3.73(4) | −2.60(4) |
| | Occ (%) | Mn 85(8) Sb 10(1) | Mn 100.0(5) | Mn 87.5(5) Sb 11.7(5) |
| | $\mu$ ($\mu_B$) | 4.52(3) | 4.11(5) | 3.98(4) |
| B | $b$ (fm) | 4.62(2) | 5.33(4) | 4.20(4) |
| | Occ (%) | Sb 90.0(2) Mn 9.4(9) | Sb 95.5(4) | Sb 81.6(6) Mn 12.5(5) |
| | $\mu$ ($\mu_B$) | 0 | 0 | 3.98(4) |
| C | $b$ (fm) | 5.68(5) | 10.39(4) | 9.00(12) |
| | Sb (%) | Pd 95.0(5) Mn 5.0(5) | Ni 100.0(3) | Ni 85(2) Sb 6(1) |
| | $\mu$ ($\mu_B$) | 0 | 0.15(2) | 0.05(4) |
| D | $b$ (fm) | 0.03(5) | 0.14(4) | 9.00(12) |
| | (%) | Pd 0.5(8) Mn 0.0(1) | Ni 1.6(3)Sb 0.2(1) | Ni 15(2) Sb 1(1) |
| | $\mu$ ($\mu_B$) | 0 | 0 | 1.0(3) |

**Table 3.** Magnetization distributions in PdMnSb and NiMnSb determined from the polarized neutron asymmetries.

| Site | | PdMnSb | NiMnSb (A) | NiMnSb (B) |
|---|---|---|---|---|
| A | Occ (%) | Mn 85(8) Sb 10(1) | Mn 100.0(5) | Mn 87.5(5) Sb 11.7(5) |
| | $\mu$ ($\mu_B$/Mn) | 4.228(15) | 3.90(2) | 4.06(3) |
| | $g$ | 2.22(2) | 2.01(3) | 1.98(3) |
| | $e_g$ (%) | 44(2) | 41(2) | 42(2) |
| B | Occ (%) | Sb 90.0(2) Mn 9.4(9) | Sb 95.5(4) | Sb 81.6(6) Mn 12.5(5) |
| C | Sb (%) | Pd 95.0(5) Mn 5.0(5) | Ni 100.0(3) | Ni 85(2) Sb 6(1) |
| | $\mu$ ($\mu_B$/Ni, Mn) | 0.43(13) | 0.147(11) | 0.175(13) |
| D | (%) | Pd 0.5(8) Mn 0.0(1) | Ni 1.6(3)Sb 0.2(1) | Ni 15(2) Sb 1(1) |
| | $\mu$ ($\mu_B$/Ni) | 0 | 0 | 0.23(5) |
| $\mu$/FU ($\mu_B$) diffraction | | 3.63(2) | 4.05(2) | 3.70(3) |
| $\mu$/FU ($\mu_B$) magnetization | | 3.92(2) | 3.96(1) | |

magnetization distributions are expressed as

$$f_i(\mathbf{q}) = \mu_i[\langle j_0(q)\rangle_i b_i \langle j_2(q)\rangle_i + a_i A(\mathbf{q})\langle j_4(q)\rangle_i],$$

$\langle j_0(q)\rangle_i$, $\langle j_2(q)\rangle_i$ and $\langle j_4(q)\rangle_i$ are the free atom form factors for $i$ = Ni or Mn [14]; $\mu_i$ is the magnetic moment associated with atom $i$ and $b_i$ the fraction of the moment due to orbital motion in the dipole approximation [15]. The $g$-factor $g_i = 2/(1 + b_i)$. The coefficient $a_i$ measures the deviation of the distribution from spherical symmetry.

$$A(hkl) = \frac{(h^4 + k^4 + l^4) - 3(h^2k^2 + k^2l^2 + l^2h^2)}{(h^2 + k^2 + l^2)^2}$$

and $\gamma = \frac{5}{2}(a_i + 1)$ is the fraction of magnetic electrons in $e_g$ orbitals. The parameters obtained are given in table 3. They show that, as expected, almost all the moment is associated with the A(Mn) site which is very nearly spherically symmetric. There are small but probably significant moments associated with Ni atoms on the C site and in the NiMnSb(B) crystal on the D sites as well, but they were too small for either their orbital content or asymmetry to be determined. No significant ordered moment was found to be associated with the B sites. The contribution of orbital motion to the magnetic moment of Mn in NiMnSb is very small $b < 0.005$ in crystal A and −0.023(15) in crystal B; in neither of these did inclusion of the $b_{Mn}$ parameter improve the goodness of fit. In PdMnSb on the other hand $b = 0.126(10)$ and its inclusion reduced the final $\chi^2$ value by a factor of almost two.

**Table 4.** Experimental and theoretical values for spin moments in the $C1_b$ compounds NiMnSb and PdMnSb.

| | | Magnetic moment per atom ($\mu_B$) | | | |
|---|---|---|---|---|---|
| Compound | Site<br>Atom | A<br>Mn | B<br>Sb | C<br>Ni/Pd | D<br>Void |
| NiMnSb | Exp. A | 3.89(3) | 0(0.1) | 0.147(11) | 0(0.02) |
| | Exp. B | 4.10(5) | 0(0.1) | 0.175(13) | 0.034(7) |
| | Theor. | 3.705 | −0.060 | 0.264 | 0.052 |
| PdMnSb | Exp. | 3.80(4) | 0(0.1) | 0.02(1) | 0(0.1) |
| | Theor. | 4.01 | −0.110 | 0.081 | 0.037 |

## 5. Discussion

Table 4 shows the values of the moments determined from the polarized neutron data compared with those obtained in the spin polarized band calculation [4]. The value of ≈4 $\mu_B$ obtained for the Mn moment in the NiMnSb crystals is rather higher than the theoretical value whereas the C site Ni moment is significantly smaller which seems to suggest an overestimation of the degree of hybridization between the two transition metals. For PdMnSb on the other hand the observed Mn moment is significantly lower than that obtained from theory. This may be due to Mn–Sb disorder but suggests that the Fermi level intersects the higher rather than the lower part of the minority spin band. A noteworthy difference between PdMnSb and NiMnSb is that in the

former the magnetic moment per formula unit obtained from the diffraction measurements is significantly lower than that corresponding to the saturation magnetization, whereas in the latter they are nearly the same. This shows that in PdMnSb, but not in NiMnSb, there are unpaired states in the majority spin bands which are delocalized throughout the unit cell so that they do not contribute to the diffraction. In PdMnSb the C site moment determined in the experiment is significantly smaller than the theoretical value and this may well be because the moment determined using the atomic model does not include the delocalized magnetization in the atomic sphere around the C site.

The changes in the band structure of NiMnSb due to atomic disorder have been investigated in a series of electronic structure calculations in which the three elements were permutated over the four lattice sites, whilst maintaining stoichiometry [16]. Disorder of the type found in both PdMnSb and NiMnSb(B) between Mn and Sb atoms was not considered. The most important effect of disorder on the band structure was to introduce additional minority spin states within the energy range of the band gap, these states widen with increasing disorder to fill the gap, giving a strong reduction in the spin polarization at $E_F$. In the NiMnSb crystal B is was found that ≈15% of the Ni atoms occupied the ideally void D sites. The associated impurity level in the minority states was found by [16] to lie in the band gap above $E_F$ and so has little effect on the moment distribution until it widens sufficiently to include $E_F$.

The proposed band structures imply that the major contribution to the magnetic moment in both compounds is due to four unpaired majority spin electrons in the five 3d antibonding bands. Since, according to the usually accepted level scheme [4], it is a majority spin $t_{2g}$ antibonding band which is open at the Fermi surface the Mn magnetization distribution should be due to $2t_{2g}$ and $2e_g$ electrons. This implies 50% $e_g$ symmetry, significantly different from the effectively spherical symmetry (40% $e_g$) found in the experiment. If the Fermi level lies in the gap in the minority spin band, so that the magnetization is due just to unpaired electrons in the conduction band, then the results show that the empty states at the top of this band must have nearly spherical symmetry suggesting a greater participation of $e_g$ electrons than a simple interpretation of the density of states might predict. Similar polarized neutron studies of $CoS_2$ [8] and $Co_2MnSi$ [9], both predicted to be half metallic, gave evidence for a finite density of states in both the majority and minority spin bands. The present results do not require participation of minority spin states in the DOS at $E_f$, but only so long as the unoccupied states at the top of the majority spin band have approximately 40% $e_g$ character.

The form factor analysis suggests that orbital momentum makes a significant contribution to the Mn magnetization in PdMnSb although it is negligible in NiMnSb. Relativistic band structure calculations on the other hand indicate that the orbital moments in both compounds should be almost completely quenched and be negligible compared with the spin moments [17]. The experimental result shows that the radial distribution of magnetization around Mn in PdMnSb differs significantly from that in NiMnSb, being more compact than that characteristic of a free neutral Mn atom. Whilst this cannot be attributed with certainty to an orbital contribution, other possible explanations seem unlikely.

## 6. Conclusions

The site occupations and magnetization distributions in NiMnSb and PdMnSb have been determined by combining integrated intensity and polarized neutron flipping ratio measurements. The values of the atomic moments found were broadly comparable with those obtained from spin polarized band structure calculations [4]. On the other hand, the Mn magnetization in both compounds was shown to be almost completely spherically symmetric which is not consistent with a single unoccupied $t_{2g}$ state in the majority spin band.

## References


[1] Prinz G A 1999 *J. Magn. Magn. Mater.* **200** 57
[2] de Groot R A, Mueller F M, van Engen P G and Buschow K H J 1983 *Phys. Rev. Lett.* **50** 2024
[3] Youn S J and Min B I 1996 *Phys. Rev.* B **51** 10436
[4] Galanakis I, Mavropoulos Ph and Dederichs P H 2006 *J. Phys. D: Appl. Phys.* **39** 765
[5] Ishida S, Masaki T, Fujii S and Asano S 1997 *Physica* B **239** 163
[6] van der Heide P A M, Baelde W, de Groot R A, de Vroomen A R, van Engen P G and Buschow K H J 1985 *J. Phys. F: Met. Phys.* **15** L75
[7] Hanssen K E H M, Mijnarends P E and Rabou L P L M 1990 *Phys. Rev.* B **42** 1533
[8] Brown P J, Neumann K-U, Simon A, Ueno F and Ziebeck K R A 2005 *J. Phys.: Condens. Matter* **17** 1583
[9] Brown P J, Neumann K-U, Webster P J and Ziebeck K R A 2000 *J. Phys.: Condens. Matter* **12** 1827
[10] Hordequin Ch, Leli'evre-Berna E and Pierre J 1997 *Physica* B **234–236** 602
[11] Brown P J, Ziebeck K R A, Bland J A C and Webster P J 1980 *J. Phys. D: Appl. Phys.* **14** 511
[12] Webster P J and Ziebeck K R A 1988 *Landolt Boernstein Neue Serie Group III* vol 19C (Berlin: Springer) Section 1.5.5
[13] Becker P J and Coppens P 1974 *Acta Crystallogr.* A **30** 129
[14] Freeman A J and Watson R E 1961 *Acta Crystallogr.* **14** 231
[15] Marshall W and Lovesey S W 1971 *Theory of Thermal Neutron Scattering* (Oxford: Oxford University Press) chapter 6
[16] Orgassa D, Fujiwara H, Schulthess T C and Butler W H 1999 *Phys. Rev.* B **60** 13237
[17] Galanakis I 2005 *Phys. Rev.* B **71** 012413